

Spring 2020

Methods for Sensitive Detection of Magneto Optic Kerr Effect

James Creed
San Jose State University

Follow this and additional works at: https://scholarworks.sjsu.edu/etd_theses

Recommended Citation

Creed, James, "Methods for Sensitive Detection of Magneto Optic Kerr Effect" (2020). *Master's Theses*. 5092.

https://scholarworks.sjsu.edu/etd_theses/5092

This Thesis is brought to you for free and open access by the Master's Theses and Graduate Research at SJSU ScholarWorks. It has been accepted for inclusion in Master's Theses by an authorized administrator of SJSU ScholarWorks. For more information, please contact scholarworks@sjsu.edu.

METHODS FOR SENSITIVE DETECTION OF MAGNETO OPTIC
KERR EFFECT

A Thesis

Presented to

The Faculty of the Department of Physics & Astronomy

San José State University

In Partial Fulfillment

of the Requirements for the Degree

Master of Science

by

James K. Creed

May 2020

© 2020

James K. Creed

ALL RIGHTS RESERVED

The Designated Thesis Committee Approves the Thesis Titled

METHODS FOR SENSITIVE DETECTION OF MAGNETO OPTIC
KERR EFFECT

by

James K. Creed

APPROVED FOR THE DEPARTMENT OF PHYSICS & ASTRONOMY

SAN JOSÉ STATE UNIVERSITY

May 2020

Dr. Peter Beyersdorf	Department of Physics and Astronomy
Dr. Chris Smallwood	Department of Physics and Astronomy
Dr. Ranko Heindl	Department of Physics and Astronomy

ABSTRACT

METHODS FOR SENSITIVE DETECTION OF MAGNETO OPTIC KERR EFFECT

by James K. Creed

The focus of this project is to numerically model the phenomenon known as the Magneto Optic Kerr Effect, MOKE, where the interaction between light and surface in the presence of a magnetic field, results in a rotation of the polarization axis of the reflected light, and to develop a method by which to experimentally measure the strength of the interaction. The amount of polarization rotation is proportional to the strength of the magnetic field and changes in polarization can be detected using polarizing optics. This thesis project successfully develops a numerical model for MOKE and an experimental method is outlined in order to measure the change in intensity using polarizing optics.

DEDICATION

I would like to dedicate this to my parents, Debbie and Kevin Creed without whom I wouldn't have the deepest love for science that I do and my wife Sarah Creed who has supported me throughout so many years and made me believe that I can do whatever I set my mind to.

ACKNOWLEDGEMENTS

I would like to also thank my SJSU professors for putting up with me and getting me through school. Dr. Peter Beyersdorf, Dr. Ranko Heindl, Dr. Chris Smallwood, Dr. Hamill, Dr. Wharton and Dr. Switz.

TABLE OF CONTENTS

CHAPTER

1	INTRODUCTION TO THESIS	1
2	THEORY/BACKGROUND	2
2.1	Magneto-Optics	2
2.2	Jones Calculus	4
2.2.1	MOKE Material as Jones Matrix	5
2.3	Maxwell's Equations at a Non-Magnetic Boundary	7
2.3.1	Gauss' Law	7
2.3.2	Faraday's Law	8
2.3.3	Gauss' Law for Magnetism	9
2.3.4	Ampere's Law	9
2.3.5	Boundary Conditions: Summary	10
2.4	Applying the Boundary Conditions	10
2.4.1	S-Polarized Incident Light	11
2.4.2	p-polarized Incident Light	12
2.5	Maxwell Equations at Magnetic Interface	13
2.5.1	Air Glass Interface	17
2.6	Measuring Phase as Variations in Intensity	21
2.6.1	Half Wave Plate: Major Axis of Polarization Rotation	21
2.6.2	Quarter Wave Plate: Circular to Linear Polarization Conversion	22

3	NUMERICAL MODEL IN PYTHON	24
	3.0.1 Numerical Calculation Methods	25
	3.1 Results of Python Code	26
	3.2 Sensitivity Analysis	30
	3.3 Sensitivity Improvements	33
	3.3.1 Balanced Detection	33
	3.3.2 Modulated Detection	34
4	FUTURE WORK: EXPERIMENT	35
	4.1 Polarization Measurement System	35
	4.2 Interpreting Results	36
	4.3 Imaging System Design	36
5	CONCLUSION	39
 APPENDIX		
A	APPENDIX	40
	A.1 PyJones	40
	A.2 Python Code	41
	A.3 Surface Plot	42
 BIBLIOGRAPHY		
		44

LIST OF TABLES

Table

2.1	Jones Matrices and Vectors	5
-----	--------------------------------------	---

LIST OF FIGURES

Figure

2.1	Polar (a), Longitudinal (b), Transverse (c) MOKE Geometries	3
2.2	Boundary condition using Gauss' Law	7
2.3	Boundary condition using Faraday's Law	8
2.4	Reflection and transmission at an air glass interface using calculations of equations 2.7 and 2.8	17
2.5	s-polarized vs. Incident Angle: Polar orientation	19
2.6	s-polarized Versus Incident Angle: Longitudinal orientation	19
2.7	p-polarized versus Incident Angle: polar orientation ; Calculated from the Fresnel boundary equations for Polar orientation	20
2.8	p-polarized Versus Incident Angle: longitudinal orientation ; Calcu- lated from the Fresnel boundary equations for Longitudinal orientation	20
3.1	Optical experiment that is being modeled in Python	25
3.2	Intensity vs. Quarter Wave-Plate Angle: P Polarization	27
3.3	Intensity vs. Wave-Plate Angle: S Polarization	27
3.4	S and p-polarized Versus Q: Longitudinal orientation	28
3.5	S and p-polarized Versus Q: Polar orientation	29
3.6	Changes in Intensity with Increasing Magnetic Field	30
4.1	Imaging Optics	38

CHAPTER 1

INTRODUCTION TO THESIS

This thesis project studies and models the interaction between light and magnetic fields. Specifically, the focus of this thesis is to model the rotation of the major axis of polarization of light after a reflection off of a metallic material that is in the presence of a magnetic field. This effect is known as the Magneto Optic Kerr Effect, MOKE, for short, and was discovered by John Kerr in 1877. MOKE is the rotation of the major axis of polarization of light upon reflection from a magnetically active material in the presence of a magnetic field. The amount of rotation is proportional to the strength of the applied magnetic field. If an optical system is designed to measure polarization rotations by changes in intensity, then it is possible to measure the amount of intensity change due to MOKE. This thesis project numerically models the MOKE phenomenon in Python and develops an experimental method by which to detect the change in intensity due to MOKE.

CHAPTER 2

THEORY/BACKGROUND

2.1 Magneto-Optics

The term magneto-optics refers to the interaction between light and a magnetic field and how magnetic fields can be utilized to manipulate properties of light. MOKE is one specific interaction where the effect rotates the major axis of polarization of light after reflecting off of a MOKE sample in the presence of a magnetic field. A MOKE sample is a material that in the presence of a magnetic field, exhibits MOKE. For example, a thin film of nickel will be a material when in the presence of a magnetic field, will exhibit MOKE. John Kerr describes this effect as a rotation of the polarization axis in the opposite direction of the magnetizing current [2]. There are two effects that emerge when light reflects off of a magnetic surface namely magnetic circular birefringence and magnetic circular dichroism. The former is a difference in the index of refraction of the magnetic material, and the latter refers to the difference in amount of absorption depending on the polarization state. Magnetic circular dichroism converts linearly polarized light into elliptical polarization by means of introducing a phase delay between the polarization components. Circular birefringence rotates the major axis of polarization by delaying both components equally. These effects scale with the strength of the applied magnetic field however, these effects do not have equal magnitudes. The dominating effect is the rotation of the major axis of polarization and only a slight change in ellipticity for oblique incident light [2]. The focus of this thesis will be on modeling the rotation of the major axis of polarization which is measured by an

optical system that converts changes in polarization to changes in intensity.

There are three orientations of the magnetic field relative to the sample, that affects the magnitude of the polarization rotation. The three orientations are shown in Figure 2.1 where the magnetic field is either a) normal to the surface, polar, b) parallel and in the plane of incidence, longitudinal, or c) transverse where the magnetic field is parallel to the surface of reflection and perpendicular to the plane of incidence. The different geometries change the amount of polarization rotation and ellipticity for a given sample and incident light. The numerical model, as discussed in chapter 3, simulates both polar and longitudinal MOKE set ups and considers the effect of many different incident angles.

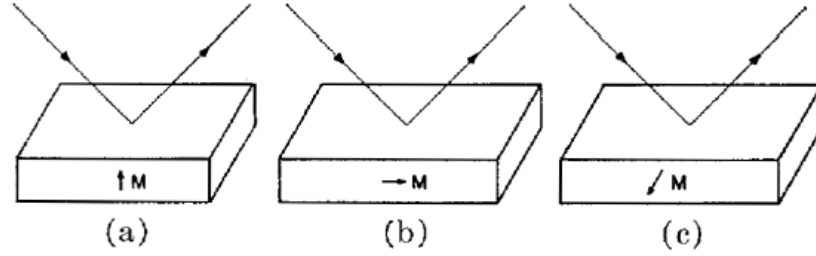


Figure 2.1: Polar (a), Longitudinal (b), Transverse (c) MOKE Geometries

Mathematically speaking, magneto optic effects arise from imaginary off-diagonal elements in the dielectric tensor of the material.

For a polar MOKE orientation, the dielectric tensor is as follows [1].

$$\frac{\epsilon}{\epsilon_0} = n^2 \begin{pmatrix} 1 & iQ & 0 \\ -iQ & 1 & 0 \\ 0 & 0 & 1 \end{pmatrix}$$

For a longitudinal MOKE orientation the following is obtained.

$$\frac{\epsilon}{\epsilon_0} = n^2 \begin{pmatrix} 1 & 0 & -iQ \\ 0 & 1 & 0 \\ iQ & 0 & 1 \end{pmatrix}$$

Where Q is a magnetic parameter that is proportional to the strength of the magnetic field and dependent on the properties of the material. n is the average index of refraction of the material. The off-diagonal elements are what give rise to the changes in polarization by affecting the phase of the polarization components of light.

2.2 Jones Calculus

The mathematical basis used to model the behavior of the components in the experiment and model the outcome of the experiment is known as Jones calculus. Jones calculus, is the mathematical formulation by which optical elements are defined as matrices, known as Jones matrices, that perform a coordinate rotation on the polarization components of the incident light which is represented by a Jones vector. To compute the end polarization state or intensity of the light after passing through a series of optics is a series of matrix multiplications, resulting in a 2x1 vector matrix representing the electric field polarization. Squaring this vector results in a vector representing the intensity. Below are the relevant Jones vectors and matrices used in this experiment and later in the paper, I will go into some sample calculations that demonstrate how to use Jones calculus as well as how some of these optical elements will be used. Table 2.1 below, shows the relevant Jones matrices and vectors for the given optical elements that are considered in the calculations.

Table 2.1: Jones Matrices and Vectors

Jones Vectors		Jones Matrices	
Polarization	Jones Vector	Optical Element	Jones Matrix
Linear Horizontal	$\begin{pmatrix} 1 \\ 0 \end{pmatrix}$	Linear Polarizer (X)	$\begin{pmatrix} 1 & 0 \\ 0 & 0 \end{pmatrix}$
Linear Vertical	$\begin{pmatrix} 0 \\ 1 \end{pmatrix}$	Linear Polarizer (Y)	$\begin{pmatrix} 0 & 0 \\ 0 & 1 \end{pmatrix}$
Circular Right	$\begin{pmatrix} 1 \\ -i \end{pmatrix}$	Half-wave Plate	$\begin{pmatrix} \cos 2\theta & \sin 2\theta \\ \sin 2\theta & -\cos 2\theta \end{pmatrix}^*$
Circular Left.	$\begin{pmatrix} 1 \\ i \end{pmatrix}$	Quarter-wave Plate	$\begin{pmatrix} 1 & 0 \\ 0 & i \end{pmatrix}^{**}$
		"Variable"-wave Plate	$\begin{pmatrix} 1 & 0 \\ 0 & e^{i\phi} \end{pmatrix}^{**}$

* Simplified from
$$\begin{pmatrix} \cos \frac{\phi}{2} + i \sin \frac{\phi}{2} \cos 2\theta & i \sin \frac{\phi}{2} \sin 2\theta \\ i \sin \frac{\phi}{2} \sin 2\theta & \cos \frac{\phi}{2} - i \sin \frac{\phi}{2} \cos 2\theta \end{pmatrix}$$

Where ϕ is rotation angle of the wave plate which in this case is zero and θ is angle relative to the fast axis.

** Jones matrices for these elements has been simplified by assuming the fast axis is horizontal.

2.2.1 MOKE Material as Jones Matrix

It is possible to develop a Jones matrix that represents a sample that will exhibit MOKE under a magnetic field using the Fresnel reflection coefficients. Since the interest is in the amplitude of the light after reflection, the Jones matrix for such a material would contain elements of the reflection coefficients for S and P polarizations along the diagonal and reflection coefficients for circular polarization

states, a combination of S and P, on the off diagonal elements. Below is the definition of the Jones matrix representing a MOKE material which has also been derived in a paper by Zak et. al. [1].

$$\text{MOKE Jones Matrix: } \begin{pmatrix} r_{ss} & r_{sp} \\ r_{ps} & r_{pp} \end{pmatrix}$$

In a numerical model, these reflection coefficients can be calculated by applying the boundary conditions as defined by Maxwell's equations to an interface between a non-magnetic, air, and a magnetic surface, the sample. Then solving the system of equations for the Fresnel coefficients. The amount of polarization rotation due to MOKE is also defined in terms of the Fresnel coefficients as the following.

$$\text{For S-Polarized incident light: } \theta_{Kerr} = \frac{r_{ps}}{r_{ss}}$$

$$\text{for P - Polarized incident light: } \theta_{Kerr} = \frac{r_{sp}}{r_{pp}}$$

Computationally the Fresnel coefficients will be solved for using the method laid out by Zak et. al. and used to estimate the amount of rotation of the axis of polarization and the intensity change due to MOKE assuming a completely ideal system.

A general approach to evaluating the boundary conditions between a magnetic and non magnetic material comes from a method developed by Zak et al. which has been generalized to solve the boundary conditions between either a non-magnetic or magnetic interface[1]. Since his method is general to any materials, applying it to an interface where the results are well defined, e.g. air to glass, is done as a verification that this method works as expected.

2.3 Maxwell's Equations at a Non-Magnetic Boundary

The Fresnel coefficient equations come from applying Maxwell's equations across the interface of two materials. Let us walk through applying Maxwell's equations between two non-magnetic materials to understand the constraints that allow us to solve for the Fresnel coefficients.

2.3.1 Gauss' Law

Let's start with applying Gauss' Law across the interface. The first step is to define a Gaussian loop between the interfaces of the materials which provide us with the behavior of the perpendicular component of the electric field. The boundary condition is derived by applying Gauss' Law, equation 2.1, across the boundary shown in Figure 2.2

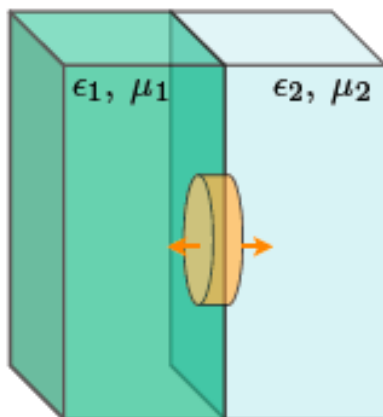


Figure 2.2: Boundary condition using Gauss' Law

Starting with Gauss' Law and expanding the equation to both sides of the boundary [5].

$$\oint \epsilon E \cdot dA = q \quad (2.1)$$

The following expression is obtained by expanding Gauss' law based on the fact that the charge inside a dielectric is zero.

$$\epsilon_1 E_{1\perp} - \epsilon_2 E_{2\perp} = 0$$

Where $E_{2\perp}$ and ϵ_2 represent the perpendicular component of the electric field and the permittivity of the second medium. Simplifying results in equation 2.2 below.

$$\epsilon_1 E_{1\perp} = \epsilon_2 E_{2\perp} \quad (2.2)$$

The result here is that the perpendicular components of the electric field must be equal across the boundary.

2.3.2 Faraday's Law

Applying Faraday's at the interface will yield the relationship between the parallel components of the electric field [5]. The boundary is shown below in Figure 2.3.

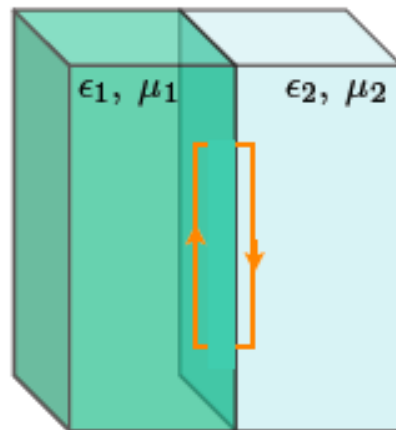


Figure 2.3: Boundary condition using Faraday's Law

$$\oint E \cdot ds = -\frac{d}{dt} \int B \cdot dA$$

The area of the loop is infinitesimal so the right side of Faraday's law becomes zero.

$$E_{1\parallel} = E_{2\parallel}$$

Where $E_{1\parallel}$ and $E_{2\parallel}$ are the parallel components of the electric field of first and second medium respectively. Applying Faraday's law at the interface shows that the parallel components of the electric field must be equal.

2.3.3 Gauss' Law for Magnetism

The magnetic field components of the incident wave at the boundary as well using Gauss' Law for magnetism [5], must be considered to find the relationship between the perpendicular components of the magnetic field. The Gaussian surface is applied at the interface as in Figure 2.1.

$$\oint B \cdot dA = 0$$

$$B_{1\perp}A - B_{2\perp}A = 0$$

$$B_{1\perp} = B_{2\perp}$$

The result is that the perpendicular components of the magnetic field, $B_{1\perp}$ and $B_{2\perp}$, at the interface must be equal.

2.3.4 Ampere's Law

Finally, applying Ampere's Law [5] at the interface and using an Amperian loop similar to the loop used for Faraday's Law, Figure (2.2). Applying this law will find the relationship between the parallel components of the magnetic field.

$$\oint \frac{B}{\mu} \cdot ds = \int J \cdot dA + \frac{d}{dt} \int \epsilon E \cdot dA$$

With no currents and in the limit that the loop approaches zero area, Ampere's

law reduces to the following.

$$\frac{B_{1\parallel}}{\mu_1}L - \frac{B_{2\parallel}}{\mu_2}L = 0$$

$$\frac{B_{1\parallel}}{\mu_1} = \frac{B_{2\parallel}}{\mu_2}$$

Finally the last boundary condition constrains the parallel components of the magnetic field to be equal at the interface.

2.3.5 Boundary Conditions: Summary

Below is a list of the four boundary conditions equations that will be applied to an incident field to understand changes in the amplitude and phase after reflection off of a dielectric medium.

Gauss' Law Parallel and Perpendicular Component Conditions.

$$\epsilon_1 E_{1\perp} = \epsilon_2 E_{2\perp} \tag{2.3}$$

$$E_{1\parallel} = E_{2\parallel} \tag{2.4}$$

Ampere's Law Parallel and Perpendicular Component Conditions.

$$B_{1\perp} = B_{2\perp} \tag{2.5}$$

$$\frac{B_{1\parallel}}{\mu_1} = \frac{B_{2\parallel}}{\mu_2} \tag{2.6}$$

2.4 Applying the Boundary Conditions

From applying both Gauss' and Faraday's Law at the interface of a dielectric, two boundary conditions have been obtained that state that the parallel and

perpendicular components of the electric field must be equal at the interface. Now that the boundary conditions are defined, the next step is to solve for the Fresnel coefficients for two interface cases. The first case is that of a non-magnetic material interface and the second is a MOKE material in the presence of a magnetic field.

2.4.1 S-Polarized Incident Light

The first step is to write the incident field as s-polarized light, meaning the polarization axis is perpendicular to the plane of incidence.

$$E_i = E_0 e^{i(kx - \omega t)}$$

$$B_i = \frac{n_i E_i}{c}$$

and the reflected wave as

$$E_r = E'_0 e^{i(k'x - \omega t)}$$

$$B_r = \frac{n_i E_r}{c}$$

and the transmitted wave as

$$E_t = E''_0 e^{i(k''x - \omega t)}$$

$$B_t = \frac{n_t E_t}{c}$$

Where n_i is incident index of refraction and n_t is the index of the material.

For S- polarized light, the tangential components of the electric and magnetic fields are continuous at the interface which results in the following expressions.

$$E_i(z = 0) + E_r(z = 0) = E_t(z = 0)$$

$$B_i(z = 0) \cos \theta_i + B_r(z = 0) \cos \theta_r = B_t(z = 0) \cos \theta_t$$

Using the definitions of the fields above, Snells law, $n_i \sin \theta_i = n_r \sin \theta_r$ and the law of reflection $\theta_i = \theta_r$,

$$n_i(E_{0r} - E_{0i}) \cos \theta_i = -n_t(E_{0r} + E_{0i}) \cos \theta_t$$

To solve for the amplitude of the reflection, the ratio of the reflected and incident electric field is calculated to obtain the Fresnel reflection coefficient for s-polarized light.

$$r_{\perp} = \frac{E_{0r}}{E_{0i}} = \frac{n_i \cos \theta_i - n_t \cos \theta_t}{n_i \cos \theta_i + n_t \cos \theta_t} \quad (2.7)$$

2.4.2 p-polarized Incident Light

Now considering when the electric field is parallel to the interface or p-polarized light, the same procedure can be repeated.

The same boundary conditions apply requiring the tangential components of the electric and magnetic field be continuous at the interface.

$$E_i(z = 0) \cos \theta_i + E_r(z = 0) \cos \theta_r = E_t(z = 0) \cos \theta_t$$

$$B_i(z = 0) + B_r(z = 0) = B_t(z = 0)$$

Which can be combined using Snell's Law ($\theta_i = \theta_r$) and $E = \frac{cB}{n}$ into

$$n_t(E_{0r} - E_{0i}) \cos \theta_i = n_i(E_{0r} + E_{0i}) \cos \theta_t$$

Finally solving for the amplitude of the reflected light results in the following equation.

$$r_{\parallel} = \frac{E_{0r}}{E_{0i}} = \frac{n_t \cos \theta_i - n_i \cos \theta_t}{n_i \cos \theta_t + n_t \cos \theta_i} \quad (2.8)$$

Now that two Fresnel reflection coefficients have been obtained for S and P polarization in a non magnetic interaction. The diagonal matrix elements in a Jones Matrix that will simulate a MOKE sample in the presence of a magnetic field. The next step is to calculate the fresnel coefficients for a magnetic sample which will be the off-diagonal terms in the MOKE Jones matrix.

2.5 Maxwell Equations at Magnetic Interface

A new method must be applied when evaluating the Fresnel coefficients at a boundary between a non-magnetic and magnetic surface. The dielectric term that is used between two non-magnetic surfaces is a scalar value since the dielectric constant does not change depending on the spatial direction the light travels in the second material. However, in a magnetic material, the dielectric constant becomes a tensor where the direction of propagation will change the value the dielectric “constant”. Applying the method developed by Zak et al follows a generalized procedure, where a matrix representing the magnetic material is used when evaluating the boundary conditions at the interface[1]. The incoming light is represented by a 4x1 vector whose elements are the polarization states. Doing so writes the polarization states in the basis of a MOKE material in the presence of a magnetic field which in this case is combinations of right and left circular polarization states. Evaluating the boundary conditions then returns a set of four independent equations that can be solved for the Fresnel coefficients which allows us to populate a 4x4 matrix containing the Fresnel coefficients in the basis of the polarization states. This process is applied for both polar and longitudinal MOKE geometries where the corresponding medium matrix is used in the calculations.

Below is the medium matrix for a magnetic and non-magnetic material, as derived by Zak et al. [1], for polar and longitudinal geometries which contains variables dependent on the incident angle of light, the index of refraction of each material and the magnetic parameter, Q . Setting $Q = 0$ will result in a medium matrix representing a non-magnetic material which in this experiment would be air. Later in this analysis, the validity of the method laid out by Zak et al., by evaluating the Fresnel coefficients at an air-glass interface where the behavior of

these coefficients is well known [1]. One underlying problem with the magnetic material analysis however, is that the behavior of the reflection and transmission coefficients is not well defined. These coefficients are unique to the magnetic material in question so evaluating the validity of that analysis will be difficult and future experimental results will help calibrate the model.

The matrix for a magnetic medium defined for polar and longitudinal geometries is shown below.

$$A_{POLAR} = \begin{pmatrix} 1 & 0 & 1 & 0 \\ \frac{i}{2}\alpha_y^2 Q & \alpha_z & \frac{i}{2}\alpha_y^2 Q & -\alpha_z \\ \frac{i}{2}\alpha_z Q N_{polar} & -N_{polar} & -\frac{i}{2}\alpha_z Q N_{polar} & -N_{polar} \\ \alpha_z N_{polar} & \frac{i}{2}Q N_{polar} & -\alpha_z N_{polar} & \frac{i}{2}Q N_{polar} \end{pmatrix}$$

$$A_{LON} = \begin{pmatrix} 1 & 0 & 1 & 0 \\ -\frac{i}{2}\frac{\alpha_y}{\alpha_z}(1 + \alpha_z^2)Q & \alpha_z & \frac{i}{2}\frac{\alpha_y}{\alpha_z}(1 + \alpha_z^2)Q & -\alpha_z \\ \frac{i}{2}\alpha_y Q N_{lon} & -N_{lon} & \frac{i}{2}\alpha_y Q N_{lon} & -N_{lon} \\ \alpha_z N_{lon} & \frac{i}{2}\frac{\alpha_y}{\alpha_z}Q N_{lon} & -\alpha_z N_{lon} & -\frac{i}{2}\frac{\alpha_y}{\alpha_z}Q N_{lon} \end{pmatrix}$$

Where α_z is equal to the following expression where n_2 is the index of refraction of the second material.

$$\alpha_z = \cos \theta_2, \alpha_y = \sin \theta_2, N_{polar} = \frac{n_2}{1 - \frac{1}{2}\alpha_z Q} N_{lon} = \frac{n_2}{1 - \frac{1}{2}\alpha_y Q}$$

Defining the electric field components in terms of the polarization components of the incident and reflected light as a polarization vector \vec{P} .

$$\vec{P} = \begin{pmatrix} E_s^i \\ E_p^i \\ E_s^r \\ E_p^r \end{pmatrix}$$

Defining each polarization component in terms of the Fresnel reflection coefficients by dividing this vector by the input s-polarized or p-polarized electric field E_s^i or E_p^i and substituting the following definitions for the Fresnel coefficients.

s-polarization

$$r_{ss} = \frac{E_s^r}{E_s^i} \quad (2.9)$$

$$r_{ps} = \frac{E_p^r}{E_s^i} \quad (2.10)$$

$$t_{ss} = \frac{E_s^i}{E_s^i} \quad (2.11)$$

$$t_{ps} = \frac{E_p^i}{E_s^i} \quad (2.12)$$

p-polarization

$$r_{pp} = \frac{E_p^r}{E_p^i} \quad (2.13)$$

$$r_{sp} = \frac{E_s^r}{E_p^i} \quad (2.14)$$

$$t_{pp} = \frac{E_p^i}{E_p^i} \quad (2.15)$$

$$t_{sp} = \frac{E_s^i}{E_p^i} \quad (2.16)$$

Now the can write \vec{P} for both polarization states as

$$\vec{P}_S = \begin{pmatrix} t_{ss} \\ t_{ps} \\ r_{ss} \\ r_{ps} \end{pmatrix}, \vec{P}_P = \begin{pmatrix} t_{pp} \\ t_{sp} \\ r_{pp} \\ r_{sp} \end{pmatrix}$$

Evaluating the fields at the boundary is the product of the material matrix A_{polar} or A_{lon} , and the polarization matrix P for each material and setting them equal as seen in equation 2.17. Where A_1 is A_2 with $Q = 0$, A_2 is the second material matrix, P_1 are the reflection components of P and P_2 are the transmission coefficients.

$$A_1 \vec{P}_1 = A_2 \vec{P}_2 \quad (2.17)$$

$$\text{s-polarization: } A_1 \begin{pmatrix} 1 \\ 0 \\ r_{ss} \\ r_{ps} \end{pmatrix} = A_2 \begin{pmatrix} t_{ss} \\ t_{ps} \\ 0 \\ 0 \end{pmatrix}, \text{p-polarization: } A_1 \begin{pmatrix} 0 \\ 1 \\ r_{sp} \\ r_{pp} \end{pmatrix} = A_2 \begin{pmatrix} t_{sp} \\ t_{pp} \\ 0 \\ 0 \end{pmatrix}$$

This operation leads to a system of four equations which can be solved for the Fresnel reflection coefficients. Solving for these coefficients is done in Python using a symbolic equation solver where these coefficients are calculated as functions of incident angle, index of the material and value of the magnetic parameter Q . Further more, these calculations are repeated for polar and longitudinal configurations by using the corresponding medium matrix A which changes slightly depending on the MOKE orientation.

2.5.1 Air Glass Interface

To test that the method developed by Zak et al. [1] works as intended, the Fresnel coefficients can be solved for a well known interface, air to glass. Evaluating at an air glass interface requires that both material matrices have their values of Q set equal to zero and that the index of the second material denoted by n_2 is now just equal to the index of glass, 1.5. The only variable here is the angle of incidence which shows up in the $\alpha_{z,y}$ term which is varied from normal incidence to parallel incident or zero to $\frac{\pi}{2}$.

In Figure 2.4 below, are the reflection and transmission coefficients as a function of incident angle for an air glass interface. The expected behavior of transmission and reflection coefficients, is observed for each input polarization state where transmission decreases as the angle of incidence is shifted away from normal to the surface.

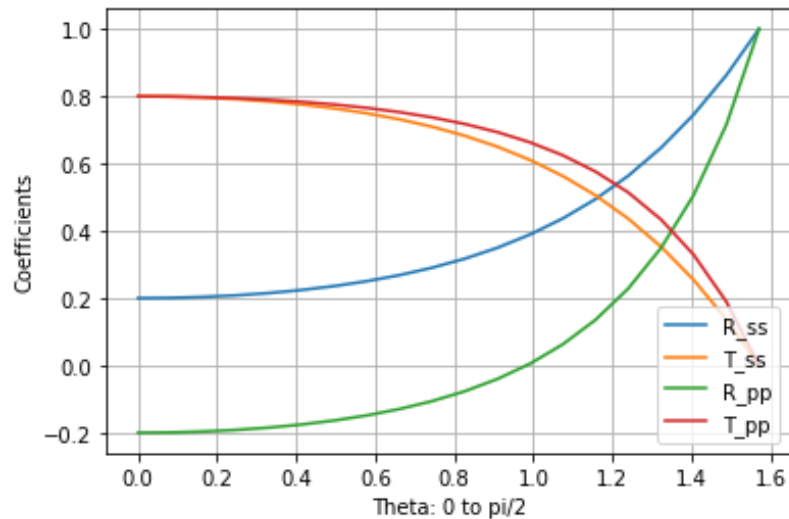


Figure 2.4: Reflection and transmission at an air glass interface using calculations of equations 2.7 and 2.8

The transmission and reflection coefficients behave as expected for an air glass

interface providing validation to the method developed by Zak et. al. The next step is to now evaluate the interface between air and a magnetically active material. Solving for the reflection coefficients in this case follows the same general procedure however the matrix that represents the second medium has non-zero values for the magnetic parameter Q . This constant serves as the independent variable in the numerical calculations as increasing the value of Q is analogous to increasing the strength of the magnetic field. A few other calculations were done in Python as well, namely varying the angle of incidence and changing the index of the second material. Figures 2.5, 2.6, 2.7, 2.8 show the calculations of the Fresnel coefficients with incident angle as the variable. Figures 2.5 and 2.6 show the Fresnel coefficients for s-polarized incident light for polar and longitudinal MOKE orientations respectively. Figures 2.7 and 2.8 consider p-polarized incident light for both MOKE orientations as well.

The circular polarization components barely change with incident angle which is expected since these components should be only dependent on the magnetization of the material. So with that in mind, the next set of calculations to be carried out would be to vary Q and observe the changes in the Fresnel reflection coefficients.

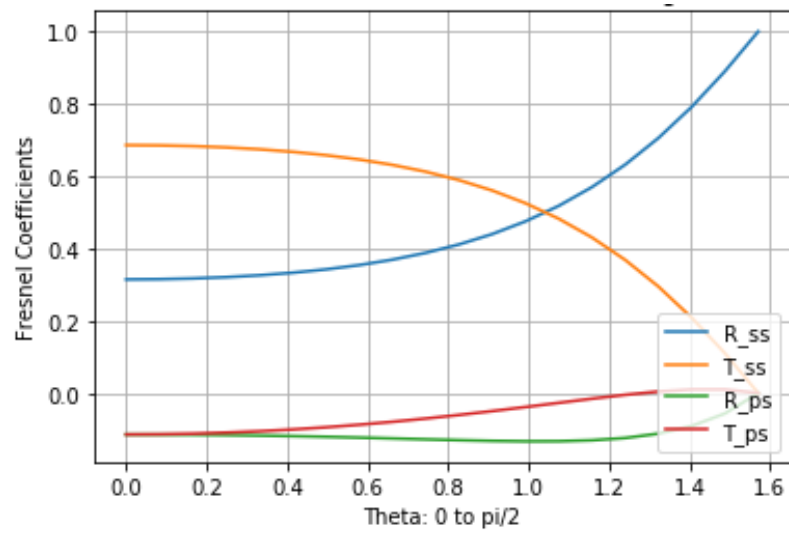


Figure 2.5: s-polarized vs. Incident Angle: Polar orientation

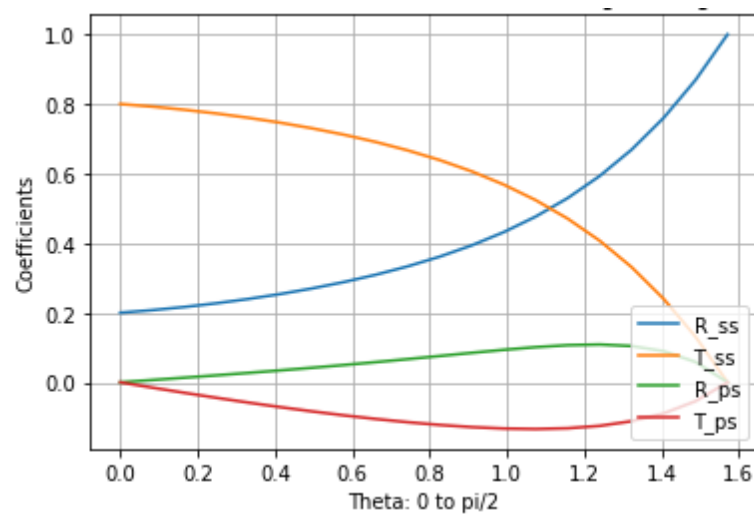


Figure 2.6: s-polarized Versus Incident Angle: Longitudinal orientation

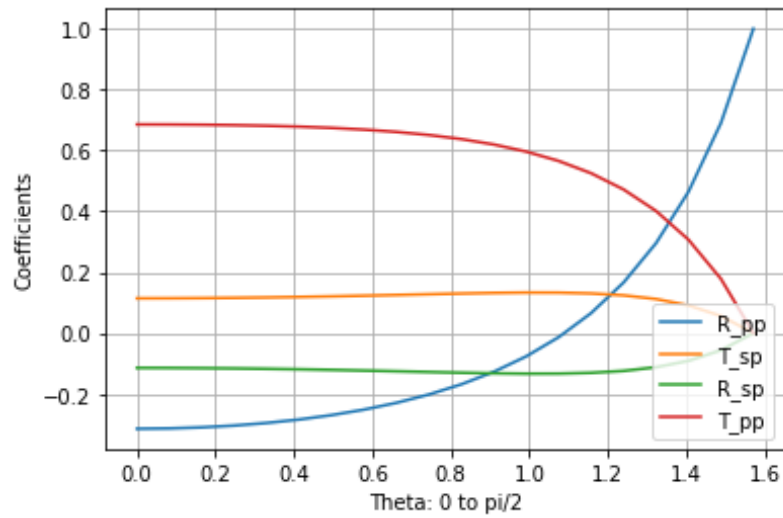


Figure 2.7: p-polarized versus Incident Angle: polar orientation ; Calculated from the Fresnel boundary equations for Polar orientation

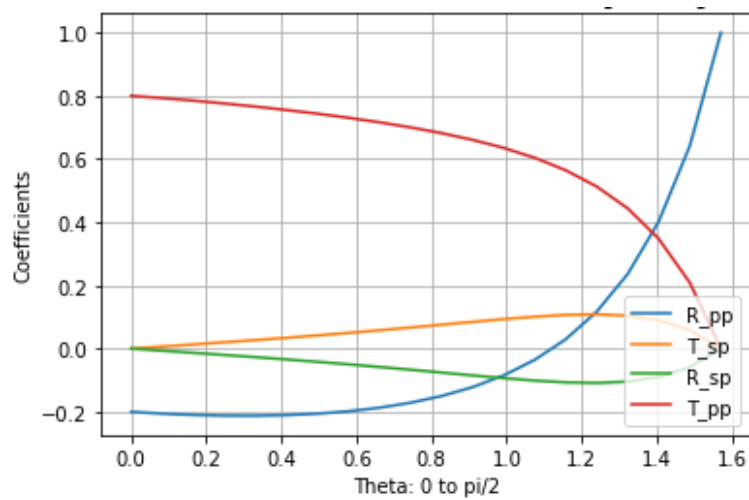


Figure 2.8: p-polarized Versus Incident Angle: longitudinal orientation ; Calculated from the Fresnel boundary equations for Longitudinal orientation

Notice that in Figures 2.5 through 2.6, there are now circular polarization components, $T_{ps,sp}$ and $R_{ps,sp}$. The presence of these circular components is expected since the MOKE material is expected to cause some slight ellipticity in the polarization state. It can also be further noted that the magnitude of these

components are much smaller than the magnitude of the normal polarization states. The take away from these results is that the numerical model is solving these boundary conditions and yielding results that are in line with intuition. These results will be used to create a MOKE Jones matrix which will accurately represent a MOKE material in the experiment.

2.6 Measuring Phase as Variations in Intensity

Measuring changes in the phase of light is not possible with a photodetector since photodetectors only measure the intensity of light. Setting up a system of polarizing optics will allow for changes in polarization to be reflected as changes in intensity which the photodetector is designed to measure. The simplest method to reflect changes in polarization as changes in intensity, is by using a polarizer. Then the intensity of light will follow Malus' law resulting in changes in intensity as the polarization angle changes. To improve the performance of the polarizer, quarter wave plates can convert the slight ellipticity of the polarization state, due to MOKE, back into linear. This will improve the extinction ratio of the polarizer meaning less of the wrong polarization will leak through.

2.6.1 Half Wave Plate: Major Axis of Polarization Rotation

Half wave plates are responsible for rotating the major axis of polarization. Below is a sample calculation demonstrating the effect of a half wave plate on the polarization of light.

$$\text{Linearly polarized light at } \theta = \begin{pmatrix} \cos \theta \\ \sin \theta \end{pmatrix}$$

and the definition of half wave plate = $\begin{pmatrix} 1 & 0 \\ 0 & -1 \end{pmatrix}$

Evaluating the effect of a half wave plate on the major axis of polarization by going through the Jones calculation.

$$\begin{pmatrix} E_x^{out} \\ E_y^{out} \end{pmatrix} = \begin{pmatrix} 1 & 0 \\ 0 & -1 \end{pmatrix} \begin{pmatrix} \cos \theta \\ \sin \theta \end{pmatrix} = \begin{pmatrix} \cos \theta \\ -\sin \theta \end{pmatrix} = \begin{pmatrix} \cos -\theta \\ \sin -\theta \end{pmatrix}$$

This results tells us that a half wave-plate rotates the axis of polarization from θ to $-\theta$ or rather two times the angle between the angle of the polarization of light and the fast axis of the wave plate. The purpose of the half wave plate is to rotate the polarization of light such that it is either parallel (p-polarized) or perpendicular (s-polarized) relative to the surface of the sample. The incident polarization angle on the MOKE sample will affect the magnitude of rotation and ellipticity due to MOKE.

Knowing that the polarization state after the magnetic sample will be some what elliptical yet the goal is to convert the polarization state back to linear. Using a quarter wave-plate, elliptical polarization is converted back into linear via introducing a phase delay to one of the polarization components effectively “catching it up” with the other component creating linearly polarized light. A sample calculation has been done to demonstrate this.

2.6.2 Quarter Wave Plate: Circular to Linear Polarization Conversion

This time, the incident light is going to be circularly polarized, a special case of elliptical, before passing through the quarter wave plate.

Right circular polarization is defined in terms of its Jones vector as:

$$R\vec{C}P = \frac{1}{\sqrt{2}} \begin{pmatrix} 1 \\ i \end{pmatrix}$$

A quarter wave plate is defined by its Jones matrix as: $\begin{pmatrix} 1 & 0 \\ 0 & i \end{pmatrix}$

$$\begin{pmatrix} E_x^{out} \\ E_y^{out} \end{pmatrix} = \begin{pmatrix} 1 & 0 \\ 0 & i \end{pmatrix} \frac{1}{\sqrt{2}} \begin{pmatrix} 1 \\ i \end{pmatrix} = \frac{1}{\sqrt{2}} \begin{pmatrix} 1 \\ -1 \end{pmatrix}$$

The end polarization state has been converted back into linear.

CHAPTER 3

NUMERICAL MODEL IN PYTHON

The numerical model developed for this experiment was done in Python. The goal of the numerical model is to model an optical system capable of measuring the MOKE rotation and for classifying the performance of the optics that would be used in said system. The performance of the wave-plates is dependent on the wavelength of light, the quality of the physical wave-plate itself and whether light is diverging or converging through the wave plate. Also manufacturing tolerances and misalignment can affect the performance of optics so an ideal case numerical model is essential. There are three variables that the numerical model needs to account for, the angle of the quarter wave-plate and half wave-plate relative to the fast axis and the strength of the magnetic field. Understanding how the MOKE signal changes with these variables will produce an ideal case that could be duplicated in a lab setting.

The experimental set up of interest in modeling is seen below in Figure 3.1. The experiment consists of a A) half wave plate, B) a variable wave plate which is modeled as a MOKE material in the presence of a magnetic field, C) a quarter wave-plate and D) a polarizing beam splitting cube. Refer to chapter 2 section 6, Measuring Phase as Variations in Intensity, for a discussion on why these specific optics were chosen.

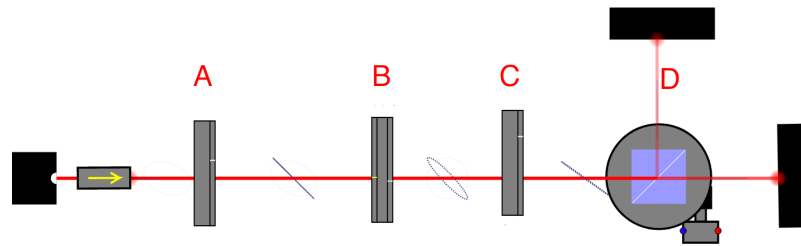


Figure 3.1: Optical experiment that is being modeled in Python

The focus of the numerical model will be to solve the Fresnel reflection equations from chapter 2 sections 3 through 5 to calculate the Fresnel coefficients as functions of incident angle and magnetic field strength. Changing the incident angle has a small effect on the strength of MOKE but the incident polarization state does change the magnitude of the effect significantly. The amount of MOKE rotation is calculated from the ratio of the Fresnel reflection coefficients corresponding to a given incident polarization. The coefficients are calculated using both P and S incident light to understand which incident polarization will result in the largest MOKE signal. The Fresnel coefficients will also make up the Jones matrix representing the MOKE material which is used in the Jones calculations to calculate the effect magnetic field strength has on intensity.

3.0.1 Numerical Calculation Methods

Jones Calculus

Calculating how a series of optics affects the output intensity and polarization is most easily done using Jones calculus. A package called PyJones provides predefined Jones matrices for the most common polarizing optics and Jones vectors for any

input electric field. Calculating output intensities is done via matrix multiplication inside a FOR loop that is iterating over the independent variable. Appendix section A.1 contains the PyJones package definitions for the various optical components.

Symbolic Equation Solving

Solving for the boundary equations across the air to magnetic material interface was done using the symbolic equation solver in Python. One of the advantages of using symbolic equations is that the solved equations can be printed out and checked for potential errors. Segments of code that demonstrate how the Python program was built in order to solve equations 2.7 through 2.14 can be found in the Appendix section A.2.

3.1 Results of Python Code

Below are the various graphs generated by the Python code that function either to calibrate the performance of the optics or to make predictions about the outcome of the experiment. Figure 3.2 shows the intensity of light as a function of the angle of the quarter wave-plate for p-polarized incident light. Since rotating the angle of the wave-plate rotates the major axis of polarization, a linear polarizer is in place set at 45 degrees before the detector. The intensity is then expected to change sinusoidally when changing the angle of the quarter wave-plate. However, the intensity should remain at a constant value when rotating the half wave plate since equal parts of either polarization state will pass through the polarizer. Figure 3.3 shows the same set of calculations but this time assuming s-incident polarization.

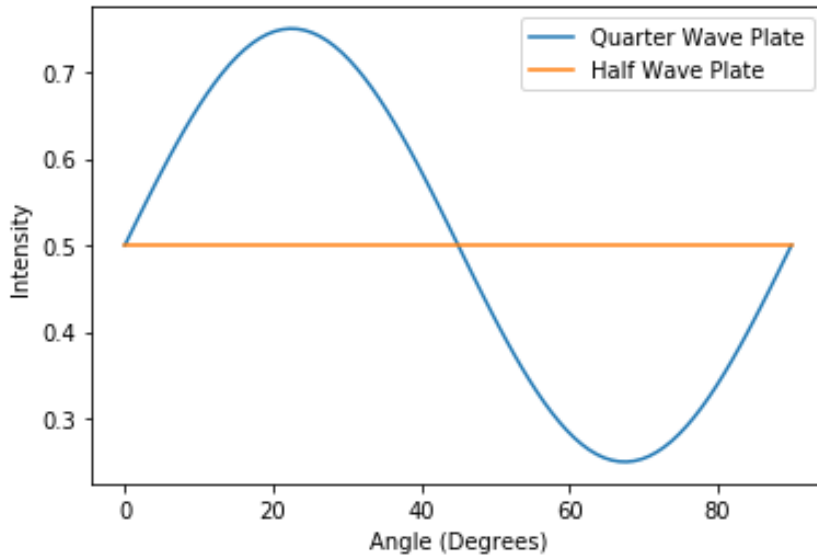


Figure 3.2: Intensity vs. Quarter Wave-Plate Angle: P Polarization

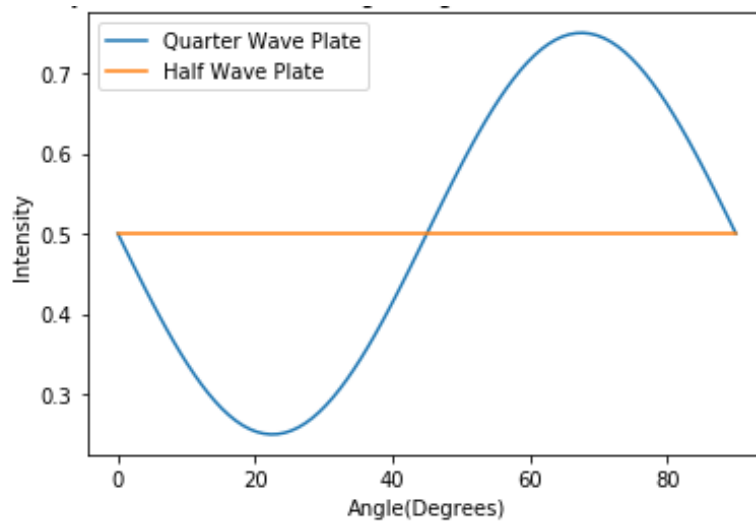


Figure 3.3: Intensity vs. Wave-Plate Angle: S Polarization

Computing the difference between the maximum and minimum intensities of the quarter wave plate plot is a change of about half of the intensity and zero for the half wave plate rotations. In practice, losses in the system will most likely attribute for more than half of the intensity being lost. The mechanical tolerances in setting

the angle of the linear polarizer at exactly 45 degrees means that the extinction ratio of the polarizer will not be ideal.

Figures 3.4 and 3.5 calculate the Fresnel reflection coefficients while changing the value of the magnetic parameter for longitudinal and polar orientations respectively. It is important to note that the coefficients regarding the circularly polarized components are equal e.g. $R_{sp} = R_{ps}$. This is why only three curves are shown when there are four different coefficients to consider.

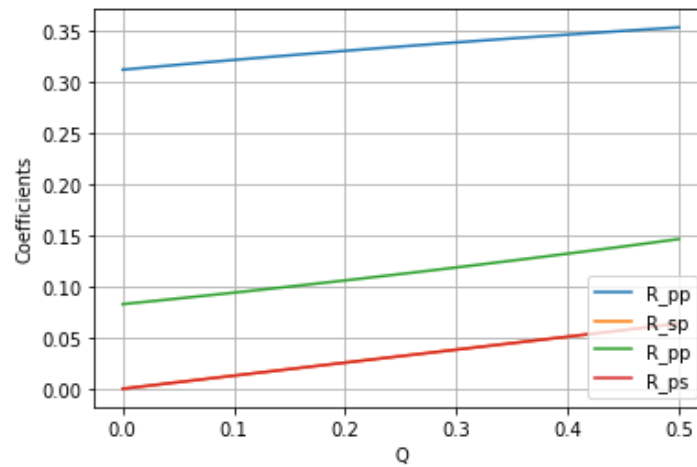


Figure 3.4: S and p-polarized Versus Q: Longitudinal orientation

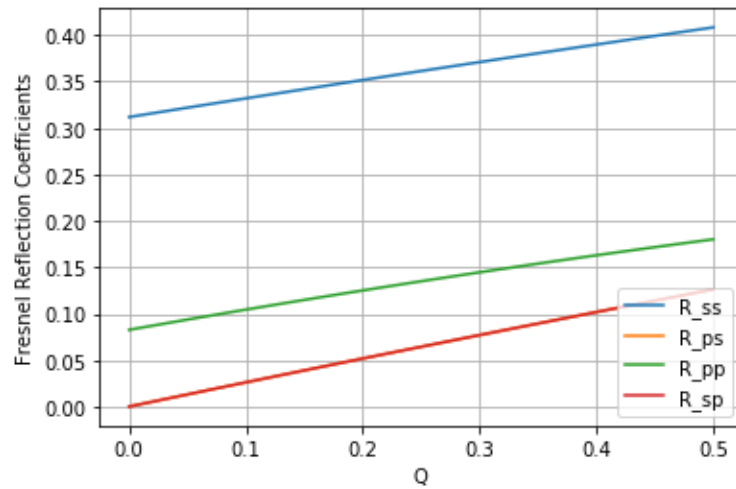


Figure 3.5: S and p-polarized Versus Q: Polar orientation

Figure 3.7, shows the results of calculating how much the intensity should change for a varying magnetic parameters. This plot is the most important result from the numerical model since the equations of these lines can be used to predict how much intensity change to expect given any arbitrary change in magnetic parameter. The next section is dedicated to using this data to understand how sensitive this optical system is to changes in magnetic parameter.

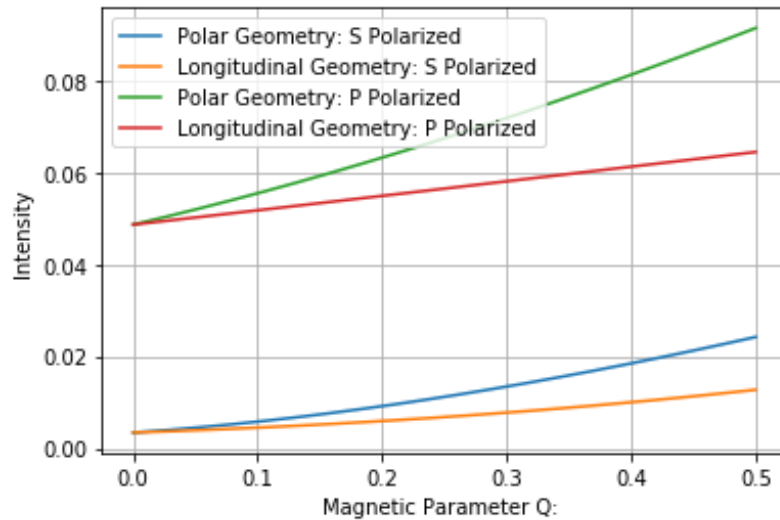


Figure 3.6: Changes in Intensity with Increasing Magnetic Field

3.2 Sensitivity Analysis

This section is dedicated to going through calculations to figure out what sort of sensitivity can be expected from a physical system set up to measure MOKE such as in figure 3.1. The sensitivity is how the system responds to a change in magnetic field. Sources of noise, the laser and the photodetector in this case, require a minimum change in signal greater than the noise level. A typical HeNe laser has a relative intensity noise of about 1% as cited from a ThorLabs HeNe laser spec sheet [4]. A photodetector has a noise spectral density reported in either amps or volts over the square root of the measurement bandwidth. The PDA10A2 silicon based photodetector from ThorLabs has a noise equivalent power spectral density of $29 \text{ pW}/\sqrt{\text{Hz}}$. The idea is to obtain an expression for ΔQ that solves for the minimum change in Q needed before a signal can be detected above these noise levels. Assuming the relationship between Q and the relative intensity is linear within the given range of Q , the slope can be approximated as the following.

$$M = \frac{\Delta V_{Pol}^O}{\Delta Q_{model}} \quad (3.1)$$

Where ΔV_{Pol}^O is the range of relative intensity values from the Python model for a given MOKE orientation, O , and incident polarization, Pol . Writing a general equation for each of the intensity versus Q lines as

$$\Delta V_m = M\Delta Q \quad (3.2)$$

Solving for ΔQ based on an relative intensity change is then calculated as

$$\Delta Q = M^{-1}\Delta V_m \quad (3.3)$$

Where ΔV_m is the change in relative intensity value as measured by a photodetector.

The other condition required is that $\Delta V_m > \Delta V_{min}$ where ΔV_{min} is the smallest detectable power. For example, a HeNe laser from ThorLabs [4], has a amplitude stability of 1% meaning that, for a direct measurement, the change in intensity due to MOKE needs to be greater than 1% of the laser power. Using the slope of each line, a minimum change in ΔQ is obtained that is required to produce a signal above the relative amplitude noise of the laser for a given MOKE orientation and incident polarization.

$$\Delta Q_S^{Polar} = .24$$

$$\Delta Q_P^{Polar} = .12$$

$$\Delta Q_S^{LON} = .31$$

$$\Delta Q_P^{LON} = .54$$

From these results, polar orientation and p-polarization incident light has the

smallest value for change Q which indicates the highest sensitivity in that configuration. However, there is not just laser noise but also noise from the photodetector that needs to be considered for an accurate value for ΔQ to be obtained.

A PDA10A2 ThorLabs silicon based photodetector has a typical noise equivalent power spectral density of $29.2 \text{ pW}/\sqrt{\text{Hz}}$ meaning it has an average noise level of $29.2 \text{ pW}[3]$ in a one second measurement. Calculating the cutoff frequency beyond which the measurement is limited by detector noise by solving the following equation for Δf .

$$\text{Noise} = 29.2 \text{ pW}/\sqrt{\text{Hz}} \times \sqrt{\Delta f} \quad (3.4)$$

$$\Delta f = \frac{\text{Noise}}{29.2 \text{ pW}/\sqrt{\text{Hz}}} \quad (3.5)$$

Solving for Δf using 1% of the 285 mW output of the laser as the noise returns 96 MHz for the cutoff frequency.

With a photodetector noise level of 29.2 pW, the required change in Q to produce a signal above that limit is calculated using equation 3.3. The results of that calculation are seen below for both polar and longitudinal orientations and s and p-polarization.

$$\Delta Q_S^{\text{Polar}} = 5.9 \times 10^{-11}$$

$$\Delta Q_P^{\text{Polar}} = 2.9 \times 10^{-11}$$

$$\Delta Q_S^{\text{LON}} = 7.8 \times 10^{-11}$$

$$\Delta Q_P^{\text{LON}} = 1.3 \times 10^{-10}$$

The sensitivity of the system drastically improves if the only source of noise is from the photodetector. In the next section, there will be a discussion on how to improve the sensitivity of the system using experimental techniques.

3.3 Sensitivity Improvements

This section is dedicated to looking at various experimental techniques that could be used in order to increase the sensitivity of an optical system to isolate the polarization rotation due to MOKE.

3.3.1 Balanced Detection

The method of balanced detection focuses on detecting the difference between two signals. In the case of this experiment, the two signals that could be measured are the two beams coming from the polarizing beam splitting cube. If the incident polarization on the cube is set to 45 degrees, then equal amount of intensity will travel down each path hence the “balanced” part of the detection. If there is a non-zero change in the major axis of polarization, then there will not be equal intensities in each beam and a non-zero signal in the difference in intensity of the beams will be obtained. Doing a balance detection also doubles the amount of signal that would be detected and eliminates the noise due to the laser. One beam coming out of the cube will contain both the background noise plus the MOKE signal and the other beam will have the background noise minus the MOKE signal. So taking the difference between these two beams would result in doubling the MOKE signal measured and suppressing any laser noise. However, the implicit assumption here is that the polarizing beam splitting cube perfectly splits the polarization components. In practice, polarizing beam splitting cubes have extinction ratios of around 30 dB meaning that one part in a thousand of the wrong polarization leaks through. So in reality, laser noise is not completely eliminated but reduced by three orders of magnitude which still drastically improves the sensitivity.

3.3.2 Modulated Detection

Another technique that can be used to increase sensitivity involves modulating the magnetic field with a current source driven by a function generator and using a lock-in amplifier to recover the MOKE signal. Modulating the current at a frequency on the order of hertz will vary the magnetic field strength over time which will also vary the amount of the polarization rotation at the same frequency. Doing this also moves the MOKE signal into a frequency where noise could be lower. For instance the low frequency noise of background room lights or $1/f$ might motivate someone to shift the MOKE signal into a different frequency channel. A lock-in amplifier can be used to recover the MOKE signal after it has been frequency shifted. The reference for the lock-in amplifier will be the frequency of the current modulator. In the absence of low frequency noise, modulation detection does not present any significant advantages when compared to balanced detection.

CHAPTER 4

FUTURE WORK: EXPERIMENT

This chapter is dedicated to designing an optical system that would be capable of measuring the polarization rotation due to MOKE. The experimental work that is needed for this thesis project was intended to be done as apart of this project. However, the COVID-19 pandemic forced San Jose State University to close and I was unable to finish the experimental side of the work. The rest of the experiment remains as future work.

4.1 Polarization Measurement System

The optical system that allows for polarization measurement utilizes the effects of wave-plates on the polarization of light to measure the changes in intensity due to MOKE. To control the incident polarization on the sample, a half wave plate is placed right after the laser source. This half-wave plate will then rotate the polarization of the laser by two times the angle between the incident polarization and the optical axis of the wave plate. The magnitude of MOKE is dependent upon the incident polarization of light on the sample. The effect is maximized when the light is p-polarized for the longitudinal MOKE orientation. The next element would be the MOKE sample which typically is a thin film of nickle. Surrounding the sample, are a pair of Helmholtz coils which apply a field parallel to the surface of the sample which activates the magneto optic properties of the material. The next optical element is a quarter wave-plate to correct the slight ellipticity in the polarization of the light coming from the sample and return it to linearly polarized

light. The angle of the linearly polarized light will depend on the amount of polarization rotation due to MOKE. The polarizer is set to 45 degrees which makes the system the most sensitive to changes in intensity.

4.2 Interpreting Results

Without an explicit expression for the magnetic parameter as a function of magnetic field strength, $Q(B)$, there needs to be a way to interpret the measurement performed in the lab. The numerical model in Python provides a model of intensity change versus the magnetic parameter, Q , but experimentally, it needs to be calibrated against a known magnetic field. Calibrating experimental data can be done by measuring the change in intensity at various magnetic field strengths. A pair of Helmholtz coils can generate a uniform field around the sample at various magnetic field strengths using a current source. Measuring the change in intensity at a few points and fitting the data will generate an expression for intensity as a function of magnetic field strength allowing for any arbitrary change in intensity to be related to a specific magnetic field strength.

4.3 Imaging System Design

The next task in this project is to image the surface of the sample onto a CCD sensor. The imaging system could be a basic two lens, 4F system that captures the nearly collimated light from the sample and then fully collimates the light before passing through the optics. There are a few constraints of this system that need to be considered when choosing the lens sizes for the imaging system. The surface of the samples range from fairly smooth and uniform to rough which means that in either case, light will scatter from the surface reducing the overall intensity

measured. This means the first lens in the imaging system needs to be as large as possible. The lenses that are used are 1 inch in diameter and will be sufficient for capturing enough light. Assuming a lens has been chosen to collect the most light, the light then needs to be collimated before passing through the rest of the optical system. The one inch diameter lenses will collimate the light at a diameter that is smaller than the diameter of the wave-plates so only two lenses are needed in order to image the sample onto the sensor.

When building an imaging system, evaluating the conditions under which vignetting will occur, provides constraints on the size of the optics that can be chosen. Checking for vignetting is done by creating a ray tracing diagram that traces rays coming from extreme points on the object. Considering a point on the object far from the optical axis, will show whether or not those rays will make it through all of the lenses. The chief ray is the ray coming from the most off center point on the object and passes through the first lens. It continues on and intersects the vertical plane passing through the second lens. If the point of intersection between the ray and the vertical plane at the second lens is larger than the diameter of the second lens, vignetting will occur. Below is the ray traced diagram, Figure 4.1, showing the chief ray coming from the object as well as a secondary ray to locate the intermediate and final image.

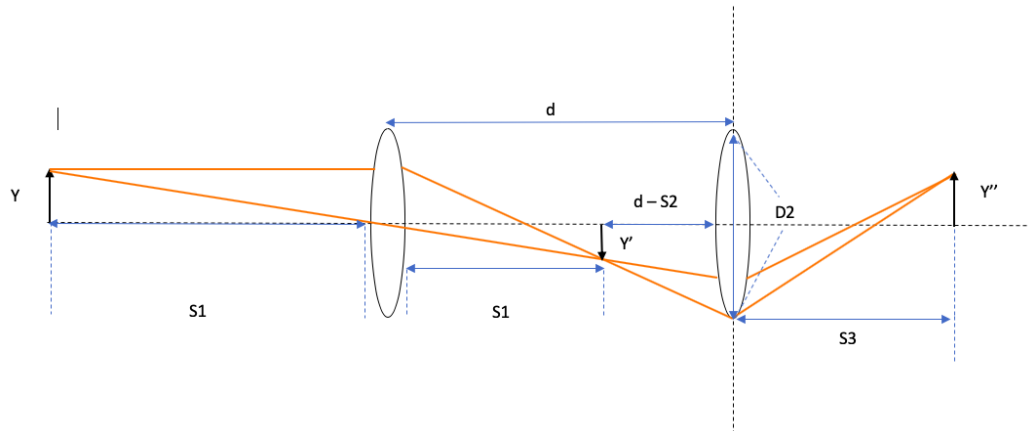


Figure 4.1: Imaging Optics

With the ray traced diagram, expressing the chief ray in terms of an equation of a line and finding the intersection point between the ray and the vertical plane passing through the second lens, yields the following equation:

$$y = \frac{m(d - S_2) - y'}{(d - S_2)} \quad (4.1)$$

$$m = \frac{y + y'}{S_2} \quad (4.2)$$

$$y = \frac{y + y'[(d - S_2) - y']}{S_2(d - S_2)} \quad (4.3)$$

A simple Excel program was created to calculate the minimum diameter of the second lens to avoid vignetting and the result is that a second lens with a diameter of one inch is sufficient to avoid vignetting. These equations can be solved for any lens combinations and is not derived specifically for the context of this experiment.

CHAPTER 5

CONCLUSION

The results of this project have laid out the foundation to build a physical system in order to measure MOKE and a few techniques in order to improve the sensitivity of the experiment. The relationship between the magnetic parameter, Q , and change in intensity has been modeled in Python. The experimental calibration to determine the relationship between Q and B which is necessary to interpret the results of the model in terms of magnetic field, remains future work. I was able to build an optical system that made use of balanced detection but could not acquire experimental data with SJSU closed due to the COVID-19 outbreak. The data that would be taken in the lab would determine the relationship between magnetic field strength and intensity change. This data can then be used along with the numerical model data to calibrate the experiment and determine the relationship between magnetic field, B , and the magnetic parameter, Q . The take away from the results of this paper are that the best sensitivity can be achieved with a polar MOKE orientation and using P incident polarized light. The model in Python also predicts that the change in relative intensity will be approximately 1 - 2%, depending on orientation and polarization, as calculated as the difference in the normalized intensity over the range of Q seen in Figure 3.7. So making a balanced detection measurement, in a polar orientation with P incident light sets up the most sensitive configuration as predicted by this analysis.

APPENDIX A

APPENDIX

A.1 PyJones

```
# Imported Optics from PyJones
from pyjones.opticalelements import Polarizer
from pyjones.opticalelements import HalfWavePlate
from pyjones.opticalelements import PolarizerVertical
from pyjones.opticalelements import QuarterWavePlate
from pyjones.opticalelements import JonesMatrix
#Imported Input Polarization States from PyJones
from pyjones.polarizations import LinearHorizontal
from pyjones.polarizations import LinearVertical
from pyjones.polarizations import CircularRight
from pyjones.polarizations import CircularLeft
```

Polarization States:

```
print LinearVertical()
out: JonesVector([0j, (1+0j)])
```

A quick note here, the printout of 1x2 matrices in Python is seen as a 2x1 instead since it has to print out the information on a single line.

```
print QuarterWavePlate(0). # zero denotes fast axis aligned
out: JonesMatrix(0.7+0j), 0j],[0j, (0+0.7j)
```

Note: The matrix here for a quarter wave plate includes the normalization factor of $1/\sqrt{2}$. Removing this factor puts this matrix into the expected form. The letter j in Python is used for denoting imaginary components of numbers instead of i .

```
print HalfWavePlate(0)
JonesMatrix([[ (1+0j), 0j], [0j, (-1+0j)]])
```

Each wave-plate Jones matrix takes one argument as input namely the angle of the fast axis relative to the plane of incidence.

A.2 Python Code

```
# The variables are first defined as symbols.
r_ss,r_ps,r_sp,r_pp,t_sp,t_pp,t_ss,t_ps,N_1,N_2 = sy.symbols ('r_ss r_ps r_sp r_pp
a_y,a_z,N,Q,n_1,n_2,a_y_2,a_z_2,a_z_1 = sy.symbols('a_y a_z N Q n_1 n_2 a_y_2 a_z_
# Setting up the Fresnel Reflection and Transmission coefficient vectors represent
Reflection_s = np.matrix([1,0,r_ss,r_ps])
R_s = Reflection_s.T # transposes to column vector
# p-polarized Incident Light
Reflection_p = np.matrix([0,1,r_sp,r_pp])
R_p = Reflection_p.T # switching to a column vector
# Transmission coefficients for S and P incident light
Transmission_s = np.matrix([t_ss,t_ps,0,0])
T_s = Transmission_s.T # switching to a column vector
Transmission_p = np.matrix([t_sp,t_pp,0,0])
T_p = Transmission_p.T
# Magnetic Material Tensor, Polar MOKE orientation
A_polar = np.matrix([[1,0,1,0],[ (1j/2)*(a_y_2**2)*Q , a_z_2 , (1j/2)*(a_y_2**2)*Q,-
```

```

# Magnetic Material Tensor, Longitudinal MOKE orientation
A_lon = np.matrix([[1,0,1,0], [(-1j/2)*(a_y_2/a_z_2)*(1+a_z_2**2)*Q , a_z_2, (1j/2)
# Air, Q =0
A_0 = np.matrix([[1,0,1,0], [0,a_z_1,0,-a_z_1], [0,-n_1,0,-n_1], [a_z_1*n_1,0,-a_z_1*
# Glass Material, Q = 0
A_0_glass = np.matrix([[1,0,1,0], [0,a_z_2,0,-a_z_2], [0,-n_2,0,-n_2], [a_z_2*n_2,0,-
# The solutions to these equations will result in a set of 4 equations and 4 unkno
F_s_glass = sy.Matrix(A_0_glass*T_s - A_0*R_s)
F_p_glass = sy.Matrix(A_0_glass*T_p - A_0*R_p)
F_S_POLAR = sy.Matrix(A_polar*T_s - A_0*R_s)
F_P_POLAR = sy.Matrix(A_polar*T_p - A_0*R_p)
F_S_LON = sy.Matrix(A_lon*T_s - A_0*R_s)
F_P_LON = sy.Matrix(A_lon*T_p - A_0*R_p)
# Solving the equations for the Fresnel coefficients
air_glass_symbolic_solution_s=sy.solve(F_s_glass, [r_ss,r_ps,t_ss,t_ps])
air_glass_symbolic_solution_p=sy.solve(F_p_glass, [r_pp,r_sp,t_pp,t_sp])
symbolic_solution_S_POLAR=sy.solve(F_S_POLAR, [r_ss,r_ps,t_ss,t_ps])
symbolic_solution_S_LON=sy.solve(F_S_LON, [r_ss,r_ps,t_ss,t_ps])
symbolic_solution_P_POLAR=sy.solve(F_P_POLAR, [r_pp,r_sp,t_pp,t_sp])
symbolic_solution_P_LON=sy.solve(F_P_LON, [r_pp,r_sp,t_pp,t_sp])

```

A.3 Surface Plot

```

THETA = np.linspace(0,5, 20)
Q_list = np.linspace(0,.5,20)
def Intensity(arrX, arrY):

```

```

returnArray=0*arrX
for i,row in enumerate(arrX):
for j, entry in enumerate(row):
    x=arrX[i][j]
    y=arrY[i][j]
    out = Polarizer(45)*QuarterWavePlate(i)*JonesMatrix([[R_SS_POLAR[j],R_PS_POLAR
    returnArray[i][j] = out.intensity
return returnArray

```

The structure of the intensity function is set up such that it can handle two variables that can be 'meshed' together and also perform the calculation using both variables at the same time. The enumerate function is responsible for calculating over all of the values of Theta and Phi simultaneously. The function will take the angle of the quarter wave-plate and the angle of the variable wave-plate (magnetic field) as input and return the intensity as expected but in a useable form for a surface plot.

BIBLIOGRAPHY

- [1] Zak, J., et al. “Universal Approach to Magneto-Optics.” *Journal of Magnetism and Magnetic Materials*, vol. 89, no. 1-2, 5 Mar. 1990, pp. 107–123., doi:10.1016/0304-8853(90)90713-z.
- [2] Lewis, E. Percival, et al. *The Effects of a Magnetic Field on Radiation ; Memoirs*. American Book Co., 1900.
- [3] “Free-Space Biased Detectors.” THORLABS, Thor Labs, www.thorlabs.com/newgrouppage9.cfm?objectgroupid=1295.
- [4] “Stabilized Red HeNe Laser.” THORLABS, THORLABS, www.thorlabs.com/newgrouppage9.cfm?objectgroupid=5281.
- [5] Jackson, John David. *Classical Electrodynamics*. N.p.: Wiley, 2016. Print.